LANGMUIR Article
Cite This: Langmuir 2018, 34, 7859−7868
pubs.acs.org/Langmuir

Controllable Synthesis of Monolayer Poly(acrylic acid) on the Channel Surface of Mesoporous Alumina for Pb(II) Adsorption

Ya-Ping Wang,[†,‡] Peng Zhou,[†] Shi-Zhong Luo,[*,†] Xue-Pin Liao,[*,‡] Bin Wang,[§] Qian Shao,[∥] Xingkui Guo,[∥] and Zhanhu Guo[*,⊥]

[†]School of Chemical Engineering and [‡]Department of Biomass Chemistry and Leather Engineering, Sichuan University, Chengdu, Sichuan 610065, PR China

[§]Engineered Multifunctional Composites (EMC) Nanotech, LLC, Knoxville, Tennessee 37934, United States

[∥]College of Chemical and Environmental Engineering, Shandong University of Science and Technology, Qingdao 266590, China

[⊥]Integrated Composites Laboratory (ICL), Department of Chemical and Biomolecular Engineering, University of Tennessee at Knoxville, Knoxville, Tennessee 37996, United States

Supporting Information

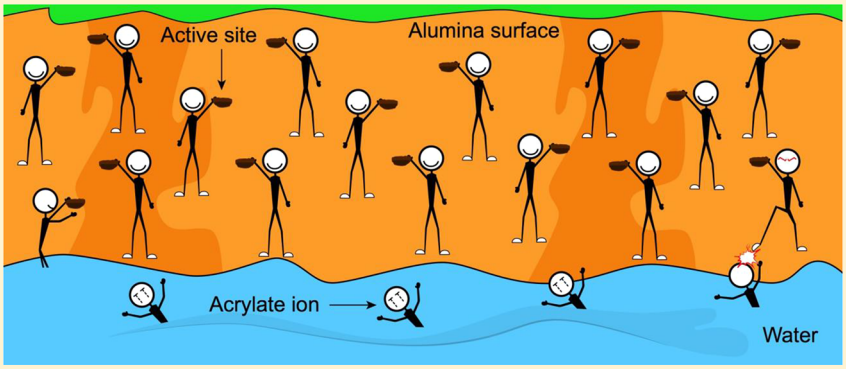

ABSTRACT: Polymer/inorganic nanocomposites exhibit special properties due to highly intimate interactions between organic and inorganic phases and thus have been deployed for various applications. Among them, nanocomposites with monolayer polymer coverage on the inorganic surface demonstrate the highest efficiency for applications. However, the controllable synthesis of the polymer monolayer in mesopores of inorganic substrates remains a challenge. In this study, poly(acrylic acid)/γ-alumina nanocomposites (PAA/alumina) were synthesized via the in situ polymerization of acrylic acid impregnated in mesopores of alumina. By applying the preneutralization of monomers, the polymerization was found to be highly controllable in generating monolayer PAA coverage. The formation of monolayers was verified by thermogravimetry, semiquantitative Fourier transform infrared spectroscopy, N_2 adsorption−desorption, and Pb(II) adsorption. Alternatively, the organic loadings of PAA/alumina composite samples could be controlled in the range of 0.2 to 1.0 equiv of monolayer, together with the linearly correlated metal ion adsorption capacity. As calculated by the complexation model, one Pb(II) is combined with two carboxylate groups of PAA. The formation of the monolayer polymer inside mesoporous oxide channels represents a method for the development of highly promising functional nanocomposites.

INTRODUCTION

Polymer/inorganic nanocomposites are a family of materials that have received tremendous attention lately because of their potential applications in biological sciences,[1] nanotechnology,[2] optoelectronics,[3] therapeutics,[4] and catalysis.[5] Well-prepared nanocomposites preserve both the hardness and thermal stability of the inorganic components and the flexibility, ductility, dielectricity, and processability of polymers.[6−8]

Mesoporous alumina is widely used in industry as a versatile adsorbent and catalyst support due to its high specific surface area, high thermal and mechanical stabilities, abundant hydroxyl groups, and low cost.[9,10] Water can be adsorbed on the γ-alumina surface through the Al(III) ion acting as a Lewis acid to accept the lone pair on the oxygen atom in water, and the formed aluminol group (Al−OH) on the surface acts as a Brønsted acid site. Additionally, the neighboring aluminol groups can form oxygen bridges and act as a Lewis acid site by losing a water molecule. Both the Brønsted acid and Lewis acid sites can adsorb metal ions and organic matter strongly depending on the solution pH.[10] However, the surface hydroxyl group shows a lower binding ability to metal ions than that of carboxyl group or the amino group;[11] therefore, surface

Received: March 9, 2018
Revised: May 15, 2018
Published: June 4, 2018

DOI: 10.1021/acs.langmuir.8b00789
Langmuir 2018, 34, 7859−7868

functionalization can be used to improve the binding capacity of alumina.[12] In this study, poly(acrylic acid) was chosen to improve the cation adsorptivity of alumina.

Poly(acrylic acid) (PAA) is a routinely used weak anionic polyelectrolyte. Although lacking certain selectivity for cations, PAA has still been utilized as an effective adsorbent owing to the massive carboxyl groups on the side chains.[13,14] The morphology of PAA chains and the dissociation of carboxyl groups are largely influenced by the solution pH.[15] At low pH, the intrachain hydrogen bonds formed between neighboring carboxyl groups causes the molecule to adopt the coiled conformation. As the pH increases, the carboxyl groups start to ionize and repel each other to stretch the polymer chains.[16] The carboxyl groups in PAA can form more stable coordination bonds with metal ions via either the bridging bidentate or the chelating bidentate mode.[17] However, it is difficult to directly use PAA because of its high solubility in water. Thus, the loading of PAA onto an inorganic network has been extensively utilized to circumvent this obstacle.[18,19]

Three methods—impregnation, the sol–gel process, and in situ polymerization—are commonly used to prepare polymer/inorganic nanocomposites.[5,20,21] Impregnation, as an easy operation and time-saving process, is widely used to prepare nanocomposites.[22] However, the impregnation of polymers presumably follows a reptation model and thus is unfavorable to the inner-pore loading of macromolecules.[9] The sol–gel process exhibits good ability for the nanometer-level dispersion of the two phases; however, the complicated preparation process hampers its practical applications.[23] The in situ polymerization is a versatile method for the preparation of nanocomposites and has a high level of control over the physiochemical properties of the products.[24] During in situ polymerization, a certain amount of monomeric precursors was adsorbed onto the surface of the inorganic phase first, followed by a commonly controlled polymerization process. Nanocomposites can be synthesized with high organic loadings because the small size of monomers allows the organic molecules to fully diffuse into the inorganic phase.[5] Also, it is easy to modify the monomers with desired functionalities to afford specific characteristics in the products during the *in situ* polymerization.[25]

In our recent work, PAA/alumina nanocomposites were fabricated by in situ polymerization of acrylic acid in mesopores of alumina.[26,27] According to the study, PAA molecules directly covering alumina surfaces were presumed to be the most efficient sites for metal ion adsorption. Thus, it is preferred to form PAA/alumina nanocomposites with monolayer PAA coverage on alumina surfaces. Earlier, the formation of a monolayer polymer coverage on mesoporous aluminosilicate SBA-15 was reported.[28] The inorganic support was filled with furfuryl alcohol and then heated to 80 °C to undergo acid-catalyzed polymerization. The polymer was formed on the wall while the remaining monomers were evaporated at the same temperature. Carbonization of the polymer followed by removing the inorganic support would eventually afford carbon molecular sieves. Therefore, a method for the preparation of a monolayer polymer covering a porous inorganic support is highly valuable in many aspects.

Herein, we report a controllable method for the synthesis of PAA/alumina nanocomposites with monolayer organic content. The monolayer PAA coverage was then verified by TG, FT-IR, and N_2 adsorption–desorption. The formation of the monolayer polymer inside mesoporous oxide channels represents a method for the development of highly functional nanocomposites. The application of this unique structure was demonstrated for the Pb(II) adsorption from polluted water.

EXPERIMENTAL SECTION

Materials. Acrylic acid (AA), potassium persulfate (PPS), ammonium persulfate (APS), and lead nitrate were acquired from Chengdu Kelong Chemical Co. (China). 4,4′-Azobis(4-cyanovaleric acid) (V501) was purchased from Chengdu Best Chemicals Co. Ltd. (China). γ-Alumina was obtained from Tianjin Kemiou Chemical Co. (China), ground into 40–60 mesh powder, and activated at 500 °C for 3 h prior to use. Other chemical reagents were all of analytical grade. Ultrapure water was used with an electrical resistivity of 18.25 MΩ·cm^{-1}. All reagents were used without further purification unless otherwise stated.

Synthesis of Monolayer PAA/Alumina Nanocomposites. In order to obtain monolayer PAA coverage at the inner surface of mesoporous alumina channels, acrylic acid was first adjusted to an optimal degree of neutralization. Here, a solution of acrylic acid of 80% neutralization was loaded in alumina via incipient wetness impregnation. The sample was rinsed repeatedly to remove free monomer and dried overnight. V501 (with twice the amount of NaOH (in moles) in solution to facilitate dissolution) and water were added to the alumina hybrid, and then the polymerization was conducted at 65 °C for 12 h under N_2 atmosphere and quenched with ice water. The sample was then fully washed and dried at 60 °C overnight to yield the PAA/alumina nanocomposite sample. In addition, composites with different AA loadings varying from 0.2 to 2.0 monolayer equivs were also prepared using the optimized condition. The as-prepared composites were named P/Al-*N*, where *N* represents the number of equivalent PAA monolayers that we intend to obtain. The relationship between the PAA loading (Γ_{PAA}) and Pb(II) equilibrium adsorption capacity (q_e) was investigated upon varying the amount of AA added (Γ_{AA}). Each nanocomposite has been prepared in three paralleled batches, and the adsorption experiments have also been performed in triplicate.

Pb(II) Adsorption on PAA/Alumina Nanocomposites. Pb(II) adsorption on PAA/alumina nanocomposites was conducted in a batch equilibrium procedure with triplicate trials. In a typical experiment, PAA/alumina nanocomposites (0.01 ± 0.0002 g) were suspended in a Pb(II) solution (25 mL) at pH 5.0–5.1, and adsorption proceeded for 48 h at room temperature. The Pb(II) concentration after adsorption was measured with an atomic absorption spectrophotometer (AAS) (AA32DCRT, Shanghai Analytical Instrument Co., China). The Pb(II) equilibrium adsorption capacity (q_e) was calculated as follows[29]

$$q_e = \frac{(c_0 - c_e)V}{m} \quad (1)$$

in which q_e is the amount of Pb(II) adsorbed at equilibrium (mg·g^{-1}), c_0 and c_e are the concentrations of Pb(II) solution at the beginning and at equilibrium (mg·L^{-1}), respectively, m is the mass of composites (g), and V is the volume of Pb(II) solution used (L).

Effect of Polymerization Parameters. On the basis of the above-mentioned procedure, the polymerization time, acrylic acid neutralization and addition, neutralization degree, and reactant ratio were varied to examine the impact of each parameter on the formation of monolayer PAA. The formed nanocomposites were also tested for their Pb(II) adsorption capacity. The adsorption experiments have been performed in triplicate.

Characterization. *TG.* Thermogravimetry (HCT-2 differential thermal balance, Beijing Hengjiu Scientific Instrument Co.) was conducted in the range of 80–600 °C in air. The sample was initially held at 80 °C for 20 min to remove the adsorbed water. The process was monitored until the weight variation reached a level of ≤0.01 mg. The sample was then heated to 600 °C at a constant heating rate of 10 °C·min^{-1}. After temperature programming, the TG curve was differentiated and the PAA loading amount (Γ_{PAA}) was calculated on the basis of the TG and obtained DTG data.

DOI: 10.1021/acs.langmuir.8b00789
Langmuir 2018, 34, 7859–7868

FT-IR. Room-temperature Fourier transform infrared spectroscopy (PerkinElmer Spectrum Two) was conducted in the range of 4000−400 cm^{-1} using KBr pellets containing ∼2 wt % samples.

N_2 Adsorption−Desorption. The specific surface areas, total pore volumes, and average pore diameters were determined using N_2 adsorption−desorption isotherms at −196 °C, which were characterized by an automated surface area and pore size analyzer (Quantachrome NOVA 1000e). Before each measurement, the samples were degassed in vacuum at 200 °C for 3 h. The specific surface areas of samples were calculated by the Brunauer−Emmett−Teller (BET) method, and the pore size distribution and average pore diameter were determined according to the Barrett−Joyner−Halenda (BJH) method applied to desorption isotherms.

PXRD. Powder X-ray diffraction analysis was performed with a DX-2700 X-ray diffractomer (Dandong Haoyuan Instrument Co. Ltd.) with Cu Kα (40 kV, 30 mA) radiation, an angle range from 10 to 80°, and a step size of 0.03°.

FESEM and HRTEM. The morphologies of the samples were determined using an FEI Nova NanoSEM450 field emission scanning electron microscope (FESEM) operated at 5 kV. High-resolution transmission electron microscopy (HRTEM) images of samples after Pb(II) adsorption were obtained using an FEI Tecnai G2 S-Twin F20 transmission electron microscope operating at 200 kV.

GPC. The molecular weight and molecular weight distribution of as-polymerized PAA in nanocomposites were measured via Viscotek 270max gel permeation chromatography (Malvern Instruments Ltd., U.K.) equipped with a TSKgel $GMPW_{XL}$ column and RI, LA, and RA detectors. Ultrapure water containing 0.1 M $NaNO_3$ and 2 wt % NaN_3 was used as the eluent at 40 °C and 0.6 $mL{\cdot}min^{-1}$, and poly(ethylene oxide) (PEO; M_w = 27 700 and PDI = 1.03) was used as an analysis standard. Before measurement, the samples were digested via excess 6 M NaOH, neutralized to pH 7 by 1 M HNO_3, dialyzed to remove contained salts (molecular weight cutoff = 500 Da), condensed via evaporation, and filtered through 0.22 μm filter membrane to give the final solutions for characterization.

RESULTS AND DISCUSSION

Controllable Synthesis of PAA/Alumina Nanocomposites with Monolayer PAA Coverage. To monitor the formation of PAA coverage on alumina, TG results were obtained to extrapolate the PAA loadings equivalent to PAA monolayers. The PAA loading amount to form a monolayer of coverage is 341.89 $\mu g{\cdot}m^{-2}$,[26] and the PAA loading amounts of composites are converted into the equivalent PAA monolayer coverage.

During the in situ polymerization of acrylic acid to form PAA, there is no net loss of matter. Therefore, the amount of added acrylic acid was used to estimate the efficiency of polymerization inside mesopores of alumina, assuming that the acrylic acid monomers in excess of the needed amount for the formation of a monolayer were adequately rinsed off. The relationship between PAA loading and the amount of acrylic acid added is shown in Figure 1. When the acrylic acid loading was increased from 0.2 to 1.0 equiv monolayer of PAA, the obtained Γ_{PAA} of the composite materials rose linearly. Within this region, the relationship between PAA coverage in the composites Γ_{PAA} and the added amount of acrylic acid Γ_{AA} can be described by $\Gamma_{PAA} = 0.833\Gamma_{AA}$, with $R^2 = 0.9995$. Therefore, for ≤1.0 monolayer PAA coverage, the adsorbed PAA amount can be precisely controlled by the amount of acrylic acid added prior to polymerization.

Above 1.0 monolayer, the increase in Γ_{AA} led to a Γ_{PAA} plateau of only ∼1.1 equiv monolayer. The discrepancy can be interpreted with the mechanism depicted in Chart 1. When acrylate ions are used to impregnate alumina pores, the negative $-COO^-$ groups can bind to the −OH of the alumina wall via hydrogen bonding. During the incipient wetness impregnation of the ionized monomers, acrylate ions will adsorb onto the oppositely charged alumina surfaces first in order to form a monolayer coverage. Any remaining acrylate ions are squeezed within the pores of alumina, repelled by the adsorbed acrylate (Chart 1a). Extensive rinsing removes extra acrylate from the alumina's outer surface. The one-monolayer acrylate ions undergo polymerization to form the corresponding PAA monolayer, while the remaining acrylate ions residing inside alumina channels will diffuse out during the solution polymerization process. When molecular acrylic acid monomers are

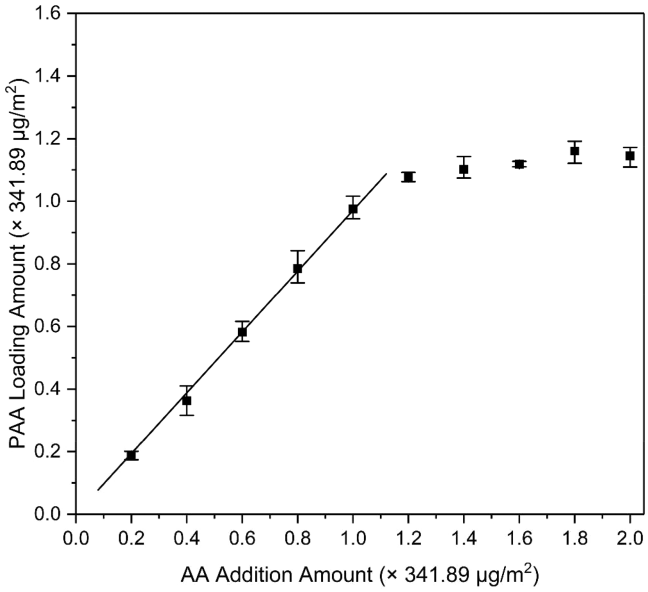

Figure 1. Relationship between obtained equivalent PAA layers in PAA/alumina nanocomposites and added acrylic acid equivalent layers.

Chart 1. Adsorption of (a) ionic acrylate and (b) molecular acrylic acid on the alumina surface

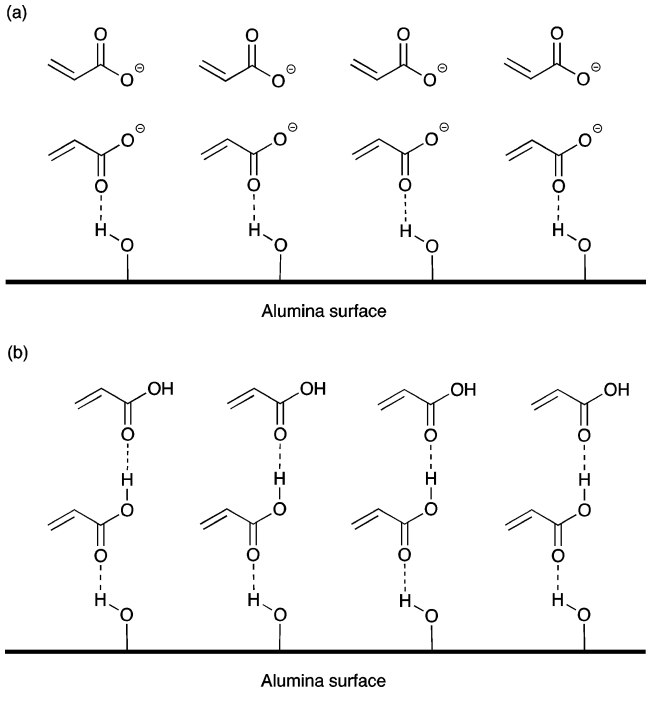

DOI: 10.1021/acs.langmuir.8b00789
Langmuir 2018, 34, 7859−7868

impregnated, one-monolayer acrylic acid molecules form hydrogen bonds with the −OH on the alumina wall surface. But more incoming acrylic acid molecules can still form hydrogen bonds with adsorbed acrylic acid (Chart 1b). In this case, PAA coverage of more than one monolayer is observed.

Characterization of PAA/Alumina Nanocomposites with Controllable PAA Coverage. In semiquantitative FT-IR spectra (Figure 2), the broad and strong peak at 1639 cm^{-1}

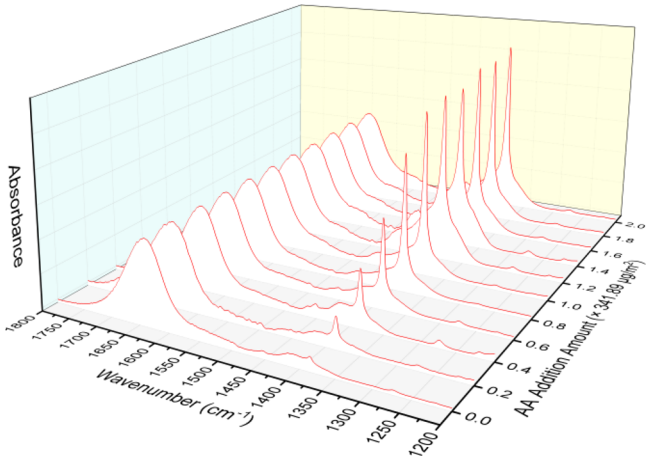

Figure 2. FT-IR spectra of composites with different acrylic acid loadings.

can be attributed to the —OH bending vibration of pristine alumina,[9,30] while the sharp peak at 1391 cm^{-1} can be attributed to the $-COO^-$ symmetric stretching vibrations of PAA.[31] The vibrational peak of the carboxylic acid group deviates from those reported in the literature (~1410 cm^{-1})[14,32,33] yet is in good agreement with that of the aqueous carboxylic acid group.[31] It is thus assumed that the as-prepared PAA monolayer resembles the carboxylic acid in aqueous solution. Normalization was performed using the −OH bending peak absorption intensity to provide a linear growth trend in the 0.2−1.0 monolayer Γ_{AA} range while reaching a plateau above 1.0 monolayer Γ_{AA} loading. The FT-IR results of PAA growth in the nanocomposites are very similar to those presented in Figure 1.

Sample P/Al-1.0 was further analyzed via TG and DTG (Figure 3). There are three peaks observed in the DTG curve of the sample. The peak at 124 °C corresponds to the removal of free and bounded water, the peak at 259 °C is from the formation of PAA anhydride, and the peak at 391 °C is attributed to the degradation of the PAA chain.[14,34,35] The PAA loading amount is calculated by subtracting the weight loss of alumina from that of composites referred to as the latter two peaks after normalization. Other samples present similar TG−DTG results as sample P/Al-1.0 despite the different weight loss, and their TG−DTG plots are thus shown in the Supporting Information as Figure S1.

On the basis of the TG curve of alumina, the percent weight loss was calculated to be ~2.71% over the whole temperature range. Bordelanne et al. has come up with an equation to calculate the fragment density[36]

$$\alpha = \frac{\Delta w}{M_{OH} \times S_A} \quad (2)$$

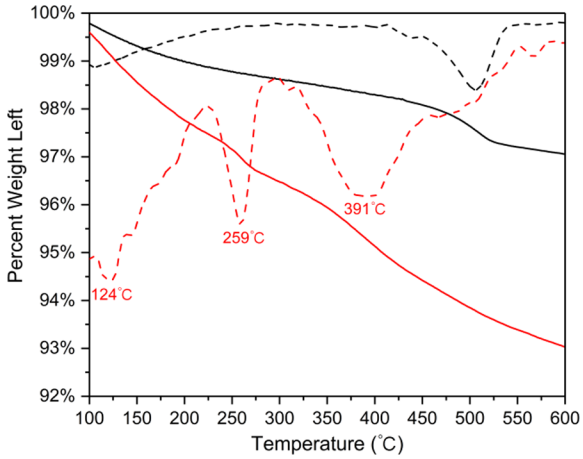

Figure 3. TG (solid lines) and DTG (dashed lines) curves of pristine alumina (presented in black) and sample P/Al-1.0 (presented in red).

where Δw is the percent weight loss of alumina, M_{OH} is the molecular weight of the hydroxyl group (17.01 $g \cdot mol^{-1}$), and S_A is the BET surface area of alumina. The surface hydroxyl group density of alumina is calculated to be ~7.88 $\mu mol \cdot m^{-2}$ or 4.74 $-OH \cdot nm^{-2}$. In our previous work, we performed a calculation to show the needed AA loading amount to form a monolayer which is ~341.89 $\mu g \cdot m^{-2}$ or 2.86 $molecule \cdot nm^{-2}$.[26] Following the above results, a hydroxyl group will occupy 0.21 nm^2 of surface area; assuming that the occupied area is a circle, the distance between two hydroxyl groups is calculated to be ~0.52 nm. In the PAA chain, the bond distance of C−C is estimated to be 0.15 nm via Chem3D software, and the C−C−C angle is 109.5°. Calculating via the law of cosines could give the distance between two carboxyl groups of 0.25 nm. Thus, there are about two AA repeat units in the distance between two hydroxyl groups to form a monolayer.

Physicochemical parameters of pristine alumina and above-mentioned composites characterized by N_2 adsorption−desorption are drawn in Figure 4. (N_2 adsorption−desorption isotherms are shown in Figure S2, and the original physicochemical data are listed in Table S1). It is observed

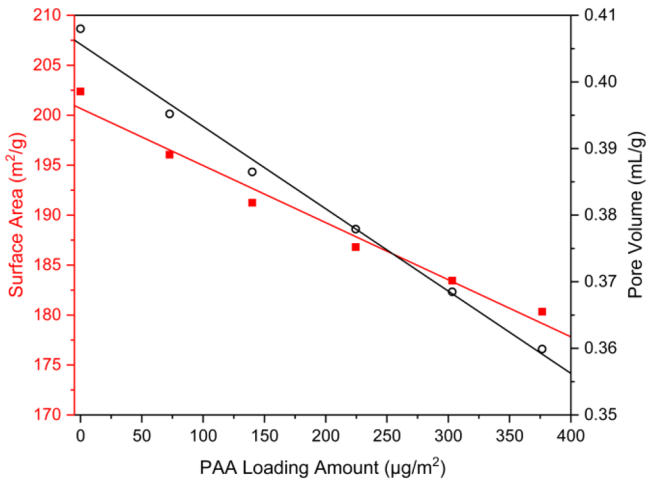

Figure 4. Relationship between two physicochemical parameters—BET surface area (red ■) and pore volume (black ○)—and PAA loading amounts in pristine alumina and PAA/alumina nanocomposites.

DOI: 10.1021/acs.langmuir.8b00789
Langmuir 2018, 34, 7859−7868

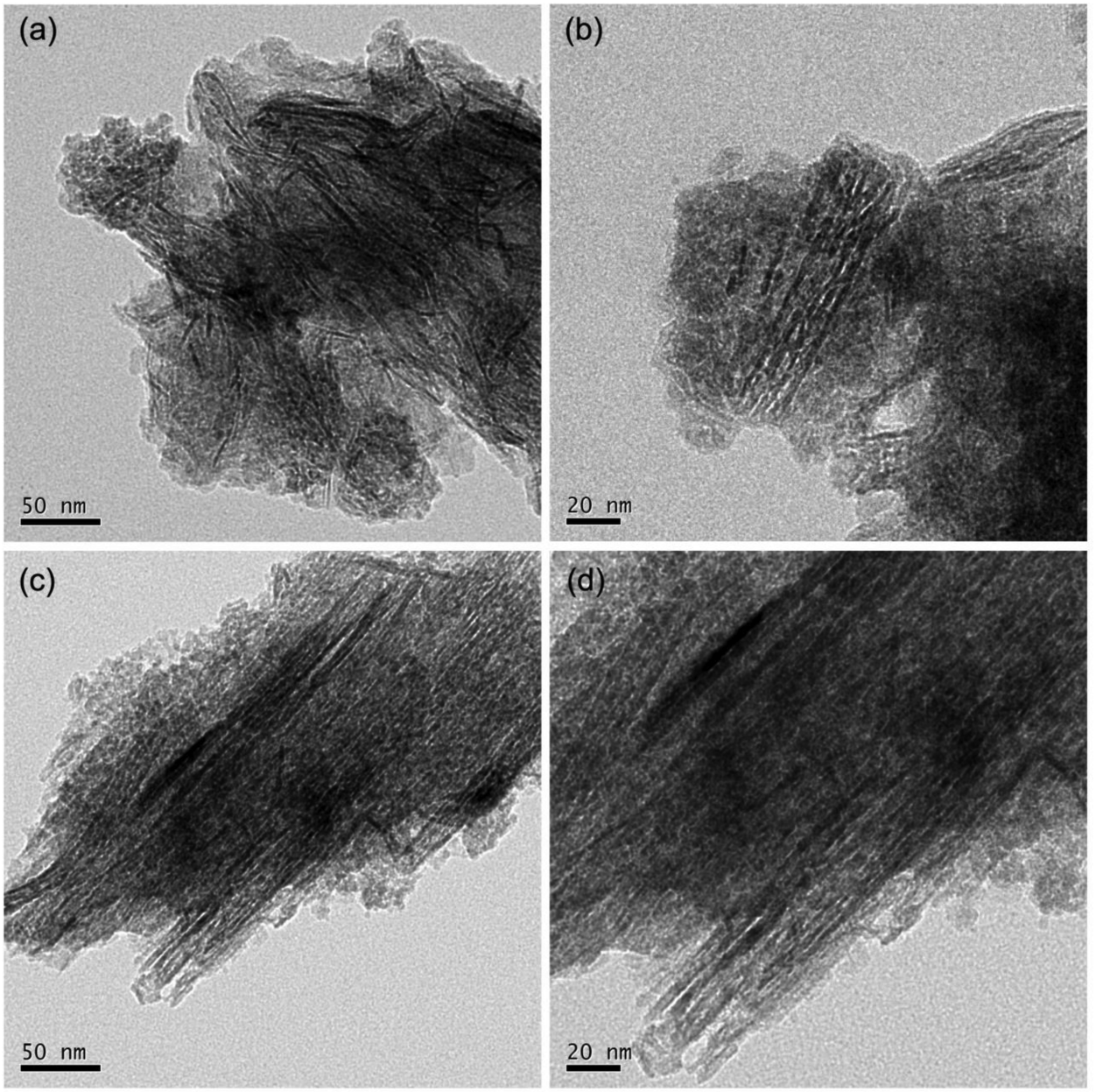

Figure 5. HRTEM images of (a and b) pristine alumina and (c and d) P/Al-1.0 with adsorbed Pb(II).

that both BET surface areas and pore volumes are linearly related to the added acrylic acid amounts (R^2 = 0.9716 for surface area and 0.9905 for pore volume). This phenomenon provides further evidence that polymerized acrylic acid is mainly retained inside the alumina pores.

We designate M_N (mg) as the mass of PAA in one gram of composite sample P/Al-*N* (measured with TG), h_N (nm) as the thickness of the polymer layer, and l (cm) as the total length of tubes in one gram of alumina, which could be calculated with eq 3.

$$l = \frac{V_A}{\pi\left(\frac{d_A}{2}\right)^2} \times 10^{14}\ \text{cm} \tag{3}$$

Experimental values are used for all parameters referring to pristine alumina, including the specific surface area (S_A), pore volume (V_A), pore diameter (d_A), and specific surface area of a composite ($S_{C,N}$):

$$S_{C,N} = \pi d_{C,N} l \times 10^3\ \text{m}^2 \tag{4}$$

On the basis of eq 4, $d_{C,N}$ could be calculated by substituting $S_{C,N}$ with corresponding values. Calculated data are used for solving the pore volume ($V_{C,N}$) and pore diameter ($d_{C,N}$) of the composite samples:

$$d_{C,N} = (d_A - 2h_N)\ \text{nm} \tag{5}$$

After the values of h_N were obtained, the density (ρ) of as-prepared PAA could be obtained using nonlinear fitting of eq 6:

$$h_N = \frac{\frac{M_N}{\rho}}{\left(\frac{1000}{M_N} - 1\right)S_A}\ \text{nm} \tag{6}$$

DOI: 10.1021/acs.langmuir.8b00789
Langmuir 2018, 34, 7859−7868

The fitting result shows that the density of as-prepared PAA in PAA/alumina is 1.16 g·cm^{-3}, slightly lower than that of commercial PAA (1.23 g·cm^{-3}).[37] We assume that this is due to the conformational difference between the PAA monolayer and bulk PAA.

PXRD peaks (Figure S3) and FESEM images (Figure S4) of PAA/alumina nanocomposites display no obvious distinctions from pristine alumina, indicating that the PAA components show no distinguishable impact on the morphology of alumina. GPC measurements show a molecular weight of as-polymerized PAA components at around 10 000 Da for the composite samples (Table S2), demonstrating the successful in situ polymerization of adsorbed AA.

Two samples, pristine alumina and P/Al-1.0, were subjected to HRTEM analysis after immersion in Pb(II) solution (Figure 5). In Figure 5a,b, adsorbed Pb(II) ions are shown as dark spots concentrated in the alumina channels, confirming that the pores are the major anchoring sites for metal ion adsorption in alumina. The shallow shades of the outer surface of alumina indicate that Pb(II) adsorbed outside the channels has largely been removed. Figure 5c,d shows that PAA/alumina shares a similar Pb(II) adsorption pattern with pristine alumina. On the basis of the statistical analysis (Figure S5), the average pore diameter exhibited a decreasing trend after the introduction of PAA. Upon close inspection, it appears that there is slightly more Pb(II) adsorption on the alumina outer surface. It is possible that some PAA molecules formed during the polymerization cover the outer surfaces of alumina and now act as metal-ion-adsorbing sites.

Pb(II) Adsorption Characteristics of PAA/Alumina Nanocomposites. Samples P/Al-*N* with N = 0.2−2.0 with an interval of 0.2 were tested for Pb(II) adsorptivity. The relationship between the amount of Pb(II) adsorbed and the amount of acrylic acid added is shown in Figure 6. Although the

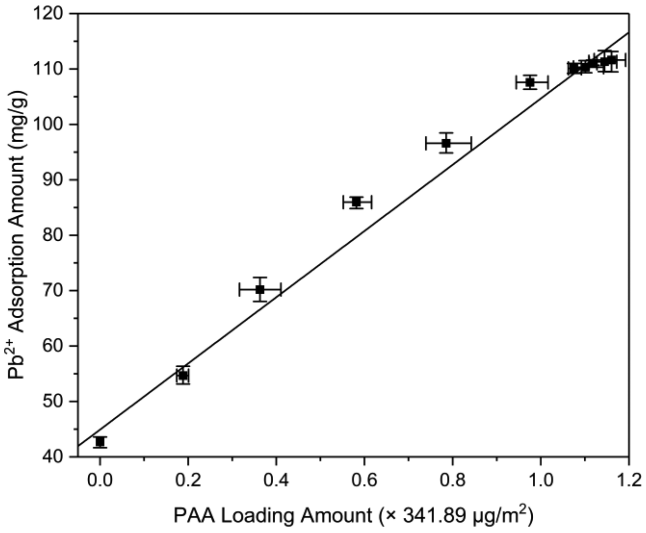

Figure 6. Relationship between the amount of Pb(II) adsorbed in PAA/alumina nanocomposites and the PAA loading amount.

latter five points were crowded due to the similar Γ_{PAA} and q_e values, the amount of Pb(II) adsorbed still shows a strong linear correlation with the PAA loading amount (q_e = 0.1748Γ_{PAA} + 44.92, R^2 = 0.9908) over the whole Γ_{PAA} range in our experiment. The intercept (44.92) represents the calculated q_e value of pristine alumina, and the slope (0.1748) gives the constant that measures the enhancement from the introduction of a certain amount of PAA.

Because a linear correlation between the Pb(II) adsorption amount and the PAA loading amount was observed, we assume that Pb(II) ions might interact with PAA through certain patterns. According to the literature, the Pb(II) ion mainly binds to carboxylic acid via complexation,[17,38,39] thus the number of carboxylate and Pb(II) ions was calculated to determine the binding properties between PAA and Pb(II). The carboxylate amounts and Pb(II) adsorption amounts could be obtained by eqs 7 and 8, respectively,

$$N_{COO^-} = \frac{\Gamma_{PAA} \times S_C \times ND}{M_{AA}}\ \mu mol \cdot g^{-1} \quad (7)$$

$$N_{Pb^{2+}} = \frac{q_C - q_A}{M_{Pb}} \times 10^3\ \mu mol \cdot g^{-1} \quad (8)$$

where Γ_{PAA} and S_C have the same meanings as mentioned above, ND represents the neutralization degree, which is 80% in this case, M_{AA} and M_{Pb} are the molar weights of acrylic acid (72.06) and lead (207.2), respectively, and q_C and q_A are the Pb(II) equilibrium adsorption amounts of composites and pristine alumina, respectively. The calculated results are presented in Table 1; the average coordination number of carboxylate to adsorbed Pb(II) ion varies from 2.15 to 2.61, with the deviation of P/Al-0.2 being mainly due to greater differences in surface area. Carboxylate could commonly form bridging mode (μ_2-η^1:η^1) or chelating mode (η^2) complexes with divalent metal ions including Pb(II) with a coordination number of 2 (Chart S1).[17,40] Our results present a coordination number that is slightly greater than 2, consistent with the literature results.

Effect of Polymerization Parameters. On the basis of characterization and analysis, we presume that the PAA monolayer coverage could be formed under our polymerization conditions. And we wonder whether the PAA monolayer could be formed when the polymerization parameters varied. Therefore, the polymerization time, acrylic acid neutralization and addition, degree of neutralization, and reactant ratio were changed to examine the impact of each parameter on the formation of monolayer PAA.

Polymerization Time. Composite samples P/Al-2h, -4h, -8h, and -12h were prepared by varying the polymerization time to 2, 4, 8, and 12 h, respectively. The relationship among Γ_{PAA}, q_e, and polymerization time is plotted in Figure 7a. It can be observed that before complete formation of the PAA monolayer there is an increased Γ_{PAA} value with an elongated reaction time, indicating a higher degree of polymerization.[41,42] P/Al-12h exhibits a Γ_{PAA} value of 338.42 $\mu g \cdot m^{-2}$, close to the value of a monolayer. Reducing the polymerization time would lead to incomplete polymerization, therefore hampering the formation of the PAA monolayer and influencing its ability to adsorb metal ions. Therefore, a polymerization time of 12 h could best form the monolayer PAA coverage.

Monomer/Initiator Ratio. In solution polymerization, PAA molar weights could be modified by changing the ratio of (acrylic acid)/(initiator).[41,43,44] Here, the reagent addition ratio was varied, and the results were shown in Figure 7b. In the Figure, the Γ_{PAA} value increases first with the increasing monomer/initiator ratio and then decreases after reaching a maximum at a ratio of 600. During the solution polymerization, initiators need to diffuse into the mesopores of alumina to

DOI: 10.1021/acs.langmuir.8b00789
Langmuir 2018, 34, 7859−7868

Table 1. Calculated Average Coordination Number of Carboxylate to Adsorbed Pb(II) Ions in PAA/Alumina Nanocomposites

sample	carboxylic ion amount (μmol·g^{-1})	Pb(II) amount (μmol·g^{-1})	average coordination number
P/Al-0.2	156.55 ± 9.21	60.21 ± 6.32	2.61 ± 0.12
P/Al-0.4	291.18 ± 30.83	135.11 ± 8.51	2.15 ± 0.09
P/Al-0.6	455.62 ± 20.68	211.26 ± 4.19	2.16 ± 0.06
P/Al-0.8	610.68 ± 33.15	262.48 ± 7.12	2.32 ± 0.06
P/Al-1.0	749.79 ± 23.11	315.55 ± 4.96	2.38 ± 0.04

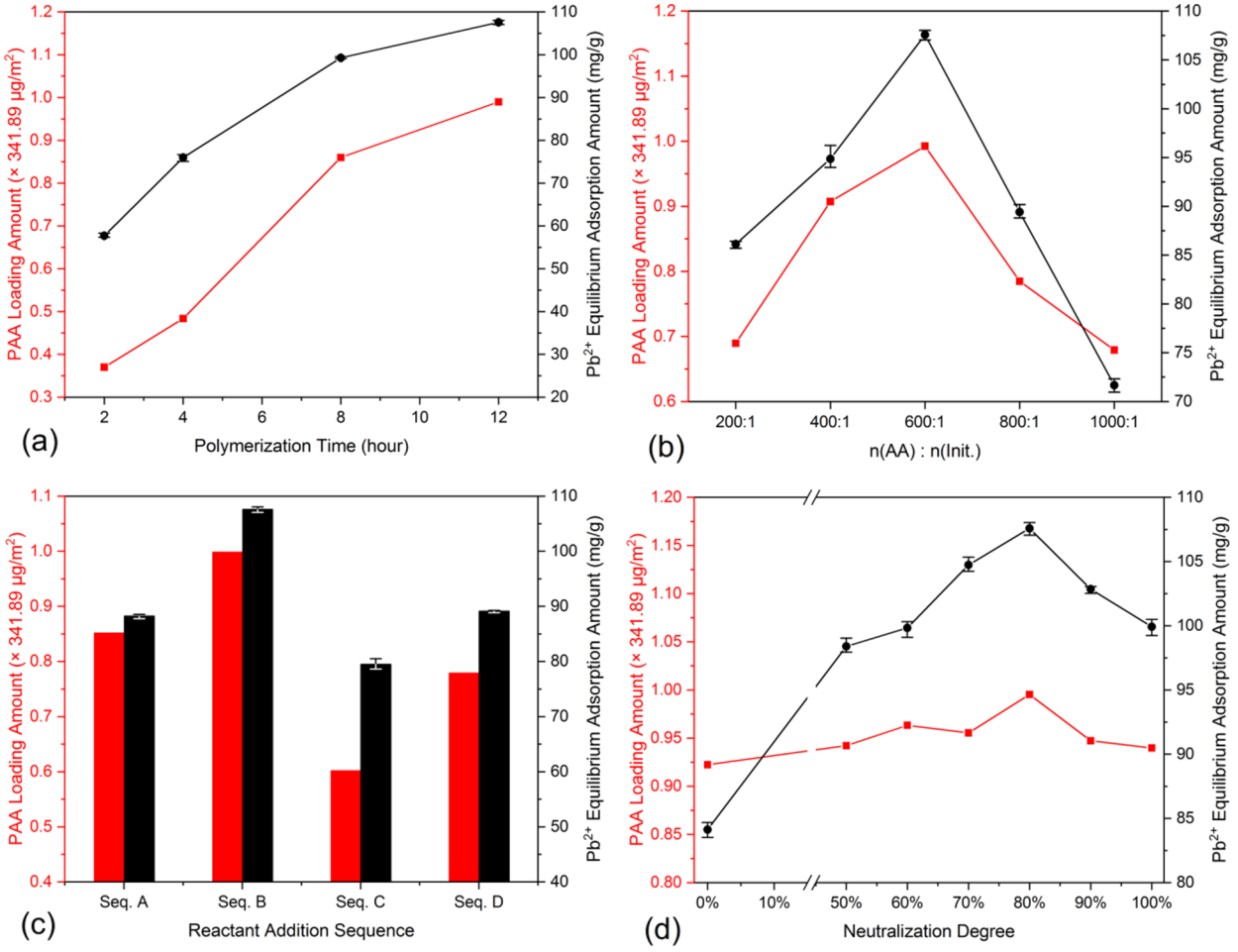

Figure 7. Effects of (a) polymerization time, (b) reactant addition ratio, (c) reactant addition sequence, and (d) neutralization degree on the PAA loading amount (presented in red) and Pb(II) equilibrium adsorption amount (presented in black).

initiate the polymerization. When the ratio is below the maximum point, enough initiators enter the pores to initiate the polymerization, forming more PAA. With more PAA chains produced, these macromolecules might block the further entry of initiators into the inner pores,[45] forming piled PAA slabs at the opening of channels. Therefore, after reaching the maximum monomer/initiator ratio, lower initiator concentration inside the pores results in a lower polymerization efficiency, thus reducing the Γ_{PAA} value. The Pb(II) equilibrium adsorption amount correlates with the Γ_{PAA} value, indicating that monolayer PAA could best adsorb metal ions. Thus, the maximum monomer/initiator of 600 is the optimal ratio for the formation of monolayer PAA coverage.

Reactant Addition Sequence. In the in situ polymerization process, the sequence addition of monomer and initiator may influence the composition of the prepared composites. In this study, four sequences that were examined are listed in Table 2, and experimental results are presented in Figure 7c. All of the addition amounts were calculated on the basis of the use of 1.000 g of alumina. If not specified, AA represents 0.07 mL of acrylic acid, NaOH represents 0.17 mL of 5 M NaOH solution, and init. represents 0.04 mL of 0.025 M V501 solution. The as-prepared samples are named P/Al-A, B, C, D. From Figure 7c, among four samples, P/Al-B had the best performance with respect to Pb(II) adsorption, followed by P/Al-D, P/Al-A, and

Table 2. Reactant Addition Sequences

sequence	impregnation 1	impregnation 2	solution reaction
A	AA + 0.29 mL of H_2O		init. + NaOH + 4.56 mL of H_2O
B	AA + NaOH + 0.12 mL of H_2O	init. + 0.32 mL of H_2O	5 mL of H_2O
C	init. + 0.32 mL of H_2O		AA + NaOH + 4.76 mL of H_2O
D	AA + NaOH + 0.12 mL of H_2O		init. + 4.96 mL of H_2O

DOI: 10.1021/acs.langmuir.8b00789
Langmuir 2018, 34, 7859−7868

P/Al-C. The difference between the preparation of P/Al-A and P/Al-D is that in P/Al-A preparation NaOH was introduced into alumina pores to neutralize preadsorbed acrylic acid while in P/Al-D preparation NaOH was directly added to acrylic acid monomer before monomer impregnation. Comparing the two samples, P/Al-D contained a lower PAA content than did P/Al-A, yet q_e of P/Al-D was higher than that of P/Al-A. We suggest in an early study that $-COO^-$ may better coordinate with metal ions than −COOH.[9] This conclusion has been suggested in other literature reports.[39,46,47] In addition, P/Al-B and P/Al-D were both impregnated first with neutralized AA monomer, but P/Al-B was then impregnated with the initiator. It can thus be assumed that the incipient wetness impregnation would lead to an even distribution of both monomer and initiator in the mesoporous channels, resulting in better formation of the PAA monolayer. Therefore, sample P/Al-B could best form the PAA monolayer and most effectively complex with Pb(II) compared to nanocomposites prepared by other reactant addition sequences.

Acrylic Acid Neutralization Degree. The optimized neutralization degree was studied to verify its impact on the metal ion complexation capability of the produced composite samples. Γ_{PAA} values of seven composite samples, P/Al-0%, -50%, -60%, -70%, -80%, -90%, and -100%, were compared, as shown in Figure 7d. All samples show relatively high Γ_{PAA} values, and P/Al-80% demonstrates slightly higher content. With regard to q_e, sample P/Al-0% has an obviously lower value than all of the other samples. This phenomenon can be correlated to the coordination pattern of carboxylate versus carboxyl groups stated above. Among the neutralized samples, q_e value grew with increasing neutralization degree until reaching 80%. After this maximum point, excess Na^+ ions remaining could lower the electrostatic attraction between carboxylate and Pb(II).[48] Therefore, nanocomposite prepared with 80% neutralized acrylic acid is considered to have the best capability to capture metal ions.

CONCLUSIONS

In this study, we synthesize PAA/alumina nanocomposites via the in situ polymerization of acrylic acid impregnating mesopores of alumina. The monolayer PAA coverage is achieved by preneutralizing AA monomer before in situ polymerization, and the PAA content in the channel of nanocomposites exhibits a loose monolayer coverage instead of piled PAA blocks. When the monomer addition amount falls in the range of 0.2 to 1.0 equiv monolayer, the preparation is featured with a controllable polymer adsorption inside alumina pores. The formation of the monolayer polymer inside mesoporous oxide channels represents a promising method for the development of monolayer functional nanocomposites.

ASSOCIATED CONTENT

Supporting Information

The Supporting Information is available free of charge on the ACS Publications website at DOI: 10.1021/acs.langmuir.8b00789.

TG−DTG curves (Figure S1), N_2 adsorption−desorption isotherms (Figure S2), PXRD figure (Figure S3), FESEM images (Figure S4), pore diameter distribution histograms (Figure S5), coordination models and surface reaction (Chart S1), original physicochemical data of N_2 adsorption−desorption (Table S1), and molecular weight and molecular weight distribution of organic components (Table S2) (PDF)

AUTHOR INFORMATION

Corresponding Authors

*(S.-Z.L.) E-mail: luosz@scu.edu.cn.
*(X.-P.L.) E-mail: xpliao@scu.edu.cn.
*(Z.G.) E-mail: zguo10@utk.edu.

ORCID

Ya-Ping Wang: 0000-0002-3308-4728
Xue-Pin Liao: 0000-0002-2704-8050
Zhanhu Guo: 0000-0003-0134-0210

Funding

The authors gratefully acknowledge financial support from the SINOPEC Maoming Company.

Notes

The authors declare no competing financial interest.

ACKNOWLEDGMENTS

We acknowledge Ming Mao, Ke-Quan Mu, and Wei Qiu from Multiphases Mass Transfer and Reaction Engineering Laboratory and Ming-Guo Zeng from Chemical Analysis Automation and the On-Line Monitoring Group of Sichuan University for their generous help on some experimental instruments and chemical reagents. We also thank Xi Yang from the Tannin Chemistry Research Group of Sichuan University for performing GPC measurements, together with Shuang-Yang Li from the Tannin Chemistry Research Group for enlightening discussions.

ABBREVIATIONS

AA, acrylic acid; PAA, poly(acrylic acid); Γ_{AA}, AA addition amount; Γ_{PAA}, PAA loading amount; q_e, Pb(II) equilibrium adsorption amount

REFERENCES

(1) Han, M.; Gao, X.; Su, J. Z.; Nie, S. Quantum-Dot-Tagged Microbeads for Multiplexed Optical Coding of Biomolecules. *Nat. Biotechnol.* **2001**, *19* (7), 631−635.

(2) Bleach, R.; Karagoz, B.; Prakash, S. M.; Davis, T. P.; Boyer, C. In Situ Formation of Polymer−Gold Composite Nanoparticles with Tunable Morphologies. *ACS Macro Lett.* **2014**, *3* (7), 591−596.

(3) Kityk, I. V.; Ebothé, J.; Fuks-Janczarek, I.; Umar, A. A.; Kobayashi, K.; Oyama, M.; Sahraoui, B. Nonlinear Optical Properties of Au Nanoparticles on Indium−tin Oxide Substrate. *Nanotechnology* **2005**, *16* (9), 1687−1692.

(4) Hirsch, L. R.; Stafford, R. J.; Bankson, J. A.; Sershen, S. R.; Rivera, B.; Price, R. E.; Hazle, J. D.; Halas, N. J.; West, J. L. Nanoshell-Mediated near-Infrared Thermal Therapy of Tumors under Magnetic Resonance Guidance. *Proc. Natl. Acad. Sci. U. S. A.* **2003**, *100* (23), 13549−13554.

(5) Choi, M.; Kleitz, F.; Liu, D.; Lee, H. Y.; Ahn, W.-S.; Ryoo, R. Controlled Polymerization in Mesoporous Silica toward the Design of Organic−Inorganic Composite Nanoporous Materials. *J. Am. Chem. Soc.* **2005**, *127* (6), 1924−1932.

(6) Zou, H.; Wu, S.; Shen, J. Polymer/Silica Nanocomposites: Preparation, Characterization, Properties, and Applications. *Chem. Rev.* **2008**, *108* (9), 3893−3957.

(7) Mizuno, M.; Takahashi, M.; Tokuda, Y.; Yoko, T. Organic−Inorganic Hybrid Material of Phenyl-Modified Polysilicophosphate Prepared through Nonaqueous Acid−Base Reaction. *Chem. Mater.* **2006**, *18* (8), 2075−2080.

DOI: 10.1021/acs.langmuir.8b00789
Langmuir 2018, 34, 7859−7868

(8) Minar, N. K.; Docampo, P.; Fattakhova-Rohlfing, D.; Bein, T. Guided in Situ Polymerization of MEH-PPV in Mesoporous Titania Photoanodes. *ACS Appl. Mater. Interfaces* **2015**, *7* (19), 10356−10364.
(9) Liu, L.; Luo, S.-Z.; Wang, B.; Guo, Z. Investigation of Small Molecular Weight Poly(Acrylic Acid) Adsorption on γ-Alumina. *Appl. Surf. Sci.* **2015**, *345*, 116−121.
(10) Kasprzyk-Hordern, B. Chemistry of Alumina, Reactions in Aqueous Solution and Its Application in Water Treatment. *Adv. Colloid Interface Sci.* **2004**, *110* (1−2), 19−48.
(11) Wang, Y.; Michel, F. M.; Levard, C.; Choi, Y.; Eng, P. J.; Brown, G. E. Competitive Sorption of Pb(II) and Zn(II) on Polyacrylic Acid-Coated Hydrated Aluminum-Oxide Surfaces. *Environ. Sci. Technol.* **2013**, *47* (21), 12131−12139.
(12) Hakimelahi, H. R.; Hu, L.; Rupp, B. B.; Coleman, M. R. Synthesis and Characterization of Transparent Alumina Reinforced Polycarbonate Nanocomposite. *Polymer* **2010**, *51* (12), 2494−2502.
(13) Liu, T.; DeSimone, J. M.; Roberts, G. W. Cross-Linking Polymerization of Acrylic Acid in Supercritical Carbon Dioxide. *Polymer* **2006**, *47* (12), 4276−4281.
(14) Parajuli, D. C.; Bajgai, M. P.; Ko, J. A.; Kang, H. K.; Khil, M. S.; Kim, H. Y. Synchronized Polymerization and Fabrication of Poly-(Acrylic Acid) and Nylon Hybrid Mats in Electrospinning. *ACS Appl. Mater. Interfaces* **2009**, *1* (4), 750−757.
(15) Saint-Aubin, K.; Poulin, P.; Saadaoui, H.; Maugey, M.; Zakri, C. Dispersion and Film-Forming Properties of Poly(Acrylic Acid)-Stabilized Carbon Nanotubes. *Langmuir* **2009**, *25* (22), 13206−13211.
(16) Grunlan, J. C.; Liu, L.; Kim, Y. S. Tunable Single-Walled Carbon Nanotube Microstructure in the Liquid and Solid States Using Poly(Acrylic Acid). *Nano Lett.* **2006**, *6* (5), 911−915.
(17) Roman, M. J.; Decker, E. A.; Goddard, J. M. Fourier Transform Infrared Studies on the Dissociation Behavior of Metal-Chelating Polyelectrolyte Brushes. *ACS Appl. Mater. Interfaces* **2014**, *6* (8), 5383−5387.
(18) Ma, Y.; Lv, L.; Guo, Y.; Fu, Y.; Shao, Q.; Wu, T.; Guo, S.; Sun, K.; Guo, Z.; Wujcik, E. K.; Guo.; et al. Porous Lignin Based Poly (Acrylic Acid)/Organo-Montmorillonite Nanocomposites: Swelling Behaviors and Rapid Removal of Pb (II) Ions. *Polymer* **2017**, *128*, 12−23.
(19) Zhou, P.; Wang, S.; Tao, C.-L.; Guo, X.-K.; Hao, L.-H.; Shao, Q.; Liu, L.; Wang, Y.-P.; Chu, W.; Wang, B.; Guo, Z. PAA/Alumina Composites Prepared with Different Molecular Weight Polymers and Utilized as Support for Nickel-Based Catalyst. *Adv. Polym. Technol.* in press, **2017**, DOI: 10.1002/adv.21908.
(20) Sumida, K.; Liang, K.; Reboul, J.; Ibarra, I. A.; Furukawa, S.; Falcaro, P. Sol−Gel Processing of Metal−Organic Frameworks. *Chem. Mater.* **2017**, *29* (7), 2626−2645.
(21) Wu, H.; Higaki, Y.; Takahara, A. Molecular Self-Assembly of One-Dimensional Polymer Nanostructures in Nanopores of Anodic Alumina Oxide Templates. *Prog. Polym. Sci.* **2018**, *77*, 95−117.
(22) Qiu, S.; Zhang, Q.; Lv, W.; Wang, T.; Zhang, Q.; Ma, L. Simply Packaging Ni Nanoparticles inside SBA-15 Channels by Co-Impregnation for Dry Reforming of Methane. *RSC Adv.* **2017**, *7* (39), 24551−24560.
(23) Yang, X.-Y.; Chen, L.-H.; Li, Y.; Rooke, J. C.; Sanchez, C.; Su, B.-L. Hierarchically Porous Materials: Synthesis Strategies and Structure Design. *Chem. Soc. Rev.* **2017**, *46* (2), 481−558.
(24) Yang, J.; Hasell, T.; Wang, W.; Li, J.; Brown, P. D.; Poliakoff, M.; Lester, E.; Howdle, S. M. Preparation of Hybrid Polymer Nanocomposite Microparticles by a Nanoparticle Stabilised Dispersion Polymerisation. *J. Mater. Chem.* **2008**, *18* (9), 998−1001.
(25) Kloust, H.; Schmidtke, C.; Feld, A.; Schotten, T.; Eggers, R.; Fittschen, U. E. A.; Schulz, F.; Pöselt, E.; Ostermann, J.; Bastús, N. G.; et al. *In Situ* Functionalization and PEO Coating of Iron Oxide Nanocrystals Using Seeded Emulsion Polymerization. *Langmuir* **2013**, *29* (15), 4915−4921.
(26) Wang, B.; Wang, Y.-P.; Zhou, P.; Liu, Z.-Q.; Luo, S.-Z.; Chu, W.; Guo, Z.-H. Formation of Poly(Acrylic Acid)/Alumina Composite via In Situ Polymerization of Acrylic Acid Adsorbed within Oxide Pores. *Colloids Surf., A* **2017**, *514*, 168−177.
(27) Wang, Y.-P.; Zhou, P.; Luo, S.-Z.; Guo, S.-J.; Lin, J.; Shao, Q.; Guo, X.-K.; Liu, Z.-Q.; Shen, J.; Wang, B.; et al. In Situ Polymerized Poly(Acrylic Acid)/Alumina Nanocomposites for Pb^{2+} Adsorption. *Adv. Polym. Technol.* in press, **2018**, DOI: 10.1002/adv.21969.
(28) Joo, S. H.; Choi, S. J.; Oh, I.; Kwak, J.; Liu, Z.; Terasaki, O.; Ryoo, R. Ordered Nanoporous Arrays of Carbon Supporting High Dispersions of Platinum Nanoparticles. *Nature* **2001**, *412* (6843), 169−172.
(29) He, S.; Zhang, F.; Cheng, S.; Wang, W. Synthesis of Sodium Acrylate and Acrylamide Copolymer/GO Hydrogels and Their Effective Adsorption for Pb^{2+} and Cd^{2+}. *ACS Sustainable Chem. Eng.* **2016**, *4* (7), 3948−3959.
(30) Gupta, S.; Ramamurthy, P. C.; Madras, G. Covalent Grafting of Polydimethylsiloxane over Surface-Modified Alumina Nanoparticles. *Ind. Eng. Chem. Res.* **2011**, *50* (11), 6585−6593.
(31) Zaman, A. A.; Tsuchiya, R.; Moudgil, B. M. Adsorption of a Low-Molecular-Weight Polyacrylic Acid on Silica, Alumina, and Kaolin. *J. Colloid Interface Sci.* **2002**, *256* (1), 73−78.
(32) Bertazzo, S.; Rezwan, K. Control of α-Alumina Surface Charge with Carboxylic Acids. *Langmuir* **2010**, *26* (5), 3364−3371.
(33) Liu, P.; Jiang, L.; Zhu, L.; Wang, A. Attapulgite/Poly(Acrylic Acid) Nanocomposite (ATP/PAA) Hydrogels with Multifunctionalized Attapulgite (Org-ATP) Nanorods as Unique Cross-Linker: Preparation Optimization and Selective Adsorption of Pb(II) Ion. *ACS Sustainable Chem. Eng.* **2014**, *2* (4), 643−651.
(34) Greenberg, A. R.; Kamel, I. Kinetics of Anhydride Formation in Poly(Acrylic Acid) and Its Effect on the Properties of a PAA-Alumina Composite. *J. Polym. Sci., Polym. Chem. Ed.* **1977**, *15* (9), 2137−2149.
(35) Moharram, M. A.; Allam, M. A. Study of the Interaction of Poly(Acrylic Acid) and Poly(Acrylic Acid-Poly Acrylamide) Complex with Bone Powders and Hydroxyapatite by Using TGA and DSC. *J. Appl. Polym. Sci.* **2007**, *105* (6), 3220−3227.
(36) Bordelanne, O.; Delville, M.-H. Metal Oxide Modification via Transition Metal Complexes: Hybrid Materials Characterizations and Potential Applications in Molecular Recognition. *Solid State Sci.* **2002**, *4* (6), 851−858.
(37) Aladdin Chemical Ltd. Poly(acrylic acid); http://www.aladdin-e.com/zh_en/p131657.html, accessed Oct 8, 2016.
(38) Campos, C. H.; Torres, C. C.; Urbano, B. F.; Rivas, B. L. Effect of the Coupling Agent on the Properties of Poly(Acrylic Acid)-Al_2O_3 Interpenetrating Hybrids and Sorption of Metal Ions. *Polym. Int.* **2015**, *64* (5), 595−604.
(39) Pal, A.; Das, D.; Sarkar, A. K.; Ghorai, S.; Das, R.; Pal, S. Synthesis of Glycogen and Poly (Acrylic Acid)-Based Graft Copolymers via ATRP and Its Application for Selective Removal of Pb^{2+} Ions from Aqueous Solution. *Eur. Polym. J.* **2015**, *66*, 33−46.
(40) Hu, M.-L.; Morsali, A.; Aboutorabi, L. Lead(II) Carboxylate Supramolecular Compounds: Coordination Modes, Structures and Nano-Structures Aspects. *Coord. Chem. Rev.* **2011**, *255* (23), 2821−2859.
(41) Loiseau, J.; Doerr, N.; Suau, J. M.; Egraz, J. B.; Llauro, M. F.; Ladaviere, C.; Claverie, J. Synthesis and Characterization of Poly-(Acrylic Acid) Produced by RAFT Polymerization. Application as a Very Efficient Dispersant of $CaCO_3$, Kaolin, and TiO_2. *Macromolecules* **2003**, *36* (9), 3066−3077.
(42) Piletska, E. V.; Guerreiro, A. R.; Whitcombe, M. J.; Piletsky, S. A. Influence of the Polymerization Conditions on the Performance of Molecularly Imprinted Polymers. *Macromolecules* **2009**, *42* (14), 4921−4928.
(43) Ladavière, C.; Dörr, N.; Claverie, J. P. Controlled Radical Polymerization of Acrylic Acid in Protic Media. *Macromolecules* **2001**, *34* (16), 5370−5372.
(44) Ji, J.; Jia, L.; Yan, L.; Bangal, P. R. Efficient Synthesis of Poly(Acrylic Acid) in Aqueous Solution via a RAFT Process. *J. Macromol. Sci., Part A: Pure Appl.Chem.* **2010**, *47* (5), 445−451.
(45) Chu, C.-W.; Higaki, Y.; Cheng, C.-H.; Cheng, M.-H.; Chang, C.-W.; Chen, J.-T.; Takahara, A. Zwitterionic Polymer Brush Grafting on Anodic Aluminum Oxide Membranes by Surface-Initiated Atom

DOI: 10.1021/acs.langmuir.8b00789
Langmuir 2018, 34, 7859−7868

Transfer Radical Polymerization. *Polym. Chem.* **2017**, *8* (15), 2309−2316.
(46) Floroiu, R. M.; Davis, A. P.; Torrents, A. Cadmium Adsorption on Aluminum Oxide in the Presence of Polyacrylic Acid. *Environ. Sci. Technol.* **2001**, *35* (2), 348−353.
(47) Tomida, T.; Hamaguchi, K.; Tunashima, S.; Katoh, M.; Masuda, S. Binding Properties of a Water-Soluble Chelating Polymer with Divalent Metal Ions Measured by Ultrafiltration. Poly(Acrylic Acid). *Ind. Eng. Chem. Res.* **2001**, *40* (16), 3557−3562.
(48) Ge, H.; Wang, S. Thermal Preparation of Chitosan−acrylic Acid Superabsorbent: Optimization, Characteristic and Water Absorbency. *Carbohydr. Polym.* **2014**, *113*, 296−303.

DOI: 10.1021/acs.langmuir.8b00789
Langmuir 2018, 34, 7859−7868